Study of Inclusive J/ψ Production in Two-Photon Collisions at LEP II with the DELPHI Detector

M. Chapkin, S.-U. Chung, P. Gavillet,
V. Obraztsov, D. Ryabchikov, A. Sokolov, S. Todorovova

Abstract

Inclusive J/ψ production in photon-photon collisions has been observed at LEP II beam energies. A clear signal from the reaction $\gamma\gamma \to J/\psi + X$ is seen. The number of observed $N(J/\psi \to \mu^+\mu^-)$ events is 36 ± 7 for the integrated luminosity of 617 pb^{-1} yielding a cross-section of $\sigma(J/\psi + X) = 45.3 \pm 18.9$ pb. Based on a study of the event shapes of different types of $\gamma\gamma$ processes in the PYTHIA program, we conclude that $(74 \pm 22)\%$ of the observed J/ψ events are due to the 'resolved' photons, the dominant contribution of which is most probably due to the gluon content of the photon.

PRELIMINARY
Contributed paper to the Summer 2002 conferences

1 Introduction

An important component of the e^+e^- collisions at LEP II energy is the two-photon fusion process. It has been pointed out that two-photon production of inclusive J/ψ's

$$e^+ + e^- \rightarrow e^+ + e^- + \gamma_1 + \gamma_2, \tag{1}$$

$$\gamma_1 + \gamma_2 \rightarrow J/\psi + X \tag{2}$$

is a sensitive channel for investigating the gluon distribution in the photon [1].

There are two important processes leading to inclusive J/ψ production. The corresponding typical diagrams are given in Fig. 1 a) and b). Less important diagrams are not considered here. The first process is described by the vector-meson dominance (VDM) model [2]

$$\gamma_1 \rightarrow c + \bar{c}, \qquad \gamma_2 \rightarrow q + \bar{q} \qquad \text{and} \qquad \gamma_1 + \gamma_2 \rightarrow J/\psi + q + \bar{q} \tag{3}$$

as shown in Fig. 1a). The vertices for γ_1 and γ_2 are connected by Pomeron exchange or diffractive dissociation of photons. The final-state parton pairs $c + \bar{c}$ and $q + \bar{q}$ are both in the state of $J^{PC} = 1^{--}$, which means that the latter is dominated by the low-mass vector mesons ρ^0, ω and ϕ but a more general inclusive hadronization of the partons may also be important.

The second process is probably described by the color-octet model [3]. It proceeds through the so-called 'resolved' contribution of the photons, in which the intermediate photons are 'resolved' into their constituent partons.

$$\gamma_1 + g_\gamma \rightarrow c + \bar{c}, \qquad \gamma_2 + g_\gamma \rightarrow q + \bar{q}, \qquad \text{and} \qquad \gamma_1 + \gamma_2 \rightarrow J/\psi + q + \bar{q} \tag{4}$$
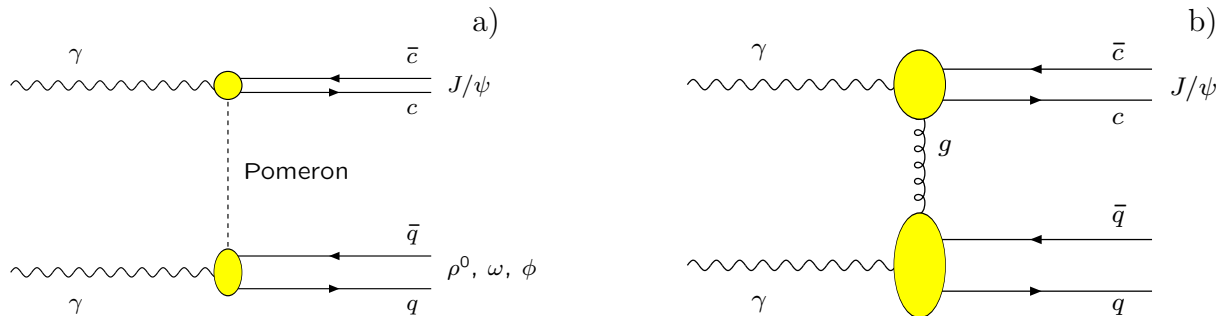
as shown in Fig. 1b).

Figure 1: Inclusive J/ψ production in $\gamma\gamma$ processes: a) through vector-meson dominance, b) via gluon content of the photon, i.e. 'resolved' contributions.

It is seen that this process requires production of a 'resolved' gluon (g_γ) from both photons. Thus, this production mechanism provides a sensitive probe of the gluon content of the photon.

The purpose of this letter is to report observation of inclusive J/ψ production from the two-photon fusion process, to give its production characteristics along with the cross-section and finally to assess the relative importance of the production processes discussed above. Section 2 describes the selection process for the event sample collected for this study. The measurement of inclusive J/ψ production in the $\mu^+\mu^-$ channel and its interpretation in terms of resolved and diffractive processes is presented in section 3 followed by a summary and conclusions.

2 Experimental Procedure

The analysis presented here is based on the data taken with the DELPHI detector [4, 5] during the years 1996–2000 for which the center of mass energies $\sqrt{s}$ for LEP ranged from 161 to 207 GeV, excluding the part of the data collected in the last period of 2000 when one of the time projection chamber (TPC) sectors was not in operation. The total integrated luminosity used in the analysis is 617 pb^{-1}.

The charged particle tracks were measured in the 1.2 T magnetic field by a set of tracking detectors including the TPC, the outer detector (OD) and the forward/backward chambers FCA and FCB. The following criteria were applied:

(a) particle momentum $p > 200$ MeV/c;

(b) relative momentum error of a track $\Delta p/p < 100\%$;

(c) impact parameter of a track, transverse to the beam axis $\Delta_{xy} < 3$ cm;

(d) impact parameter of a track, along the beam axis $\Delta_z < 7$ cm;

(e) polar angle of a track, with respect to the beam axis $10° < \theta < 170°$;

(f) track length $\ell > 30$ cm.

The neutral particles (γ, π^0, K_L^0, n) were selected by demanding that the calorimetric information, not associated with charged particle tracks, satisfy the following cuts:

(g) E(neutral) > 0.2 GeV for the electromagnetic showers unambiguously identified as photons;

(h) E(neutral) > 0.5 GeV for all the other showers;

(i) polar angle of a neutral particle tracks, with respect to the beam axis $10° < \theta < 170°$.

In order to ensure a very high trigger efficiency, the selected events were required to satisfy at least *one* of the following sets of criteria:

(j_1) one or more charged particle tracks in the barrel region ($40° < \theta < 140°$) with $p_t > 1.2$ GeV/c;

(j_2) one or more neutral particle tracks in the Forward Electromagnetic Calorimeter (FEMC) ($10° < \theta < 36°$ and $144° < \theta < 170°$) with energy greater than 10 GeV;

(j_3) the sum of the number of charged particle tracks in the barrel with $p_t > 1$ GeV/c, of charged particle tracks in the forward region ($10° < \theta < 40°$ or $140° < \theta < 170°$) with $p_t > 2$ GeV/c and of neutral particle track in the FEMC with $E > 7$ GeV is greater than one;

(j_4) the sum of the number of charged particle tracks in the barrel with $p_t > 0.5$ GeV/c of charged particle tracks in the forward region with $p_t > 1$ GeV/c and of neutral particle tracks in the FEMC with $E > 5$ GeV is greater than four.

The trigger efficiency for the events which passed the above requirements is bigger than 98%.

The hadronic two-photon events are characterized by a low visible invariant mass. Consequently, the following additional cuts were applied:

(k) the visible invariant mass, W_{vis}, calculated from the four-momentum vectors of the measured charged and neutral particle tracks, is less than 35 GeV/c^2;

(l) the number of charged particle tracks N_{ch} satisfies $4 \leq N_{\mathrm{ch}} \leq 30$;

(m) the sum of the transverse energy components with respect to the beam direction for all charged particle tracks ($\sum E_T^{\mathrm{vis}}$) is greater than 3 GeV.

The comparison of the W_{vis} distributions—after the cuts on N_{ch} and $\sum E_T^{\mathrm{vis}}$ —both for the data and the events simulated by PYTHIA (Fig. 2) shows that the cut $W_{\mathrm{vis}} \leq 35$

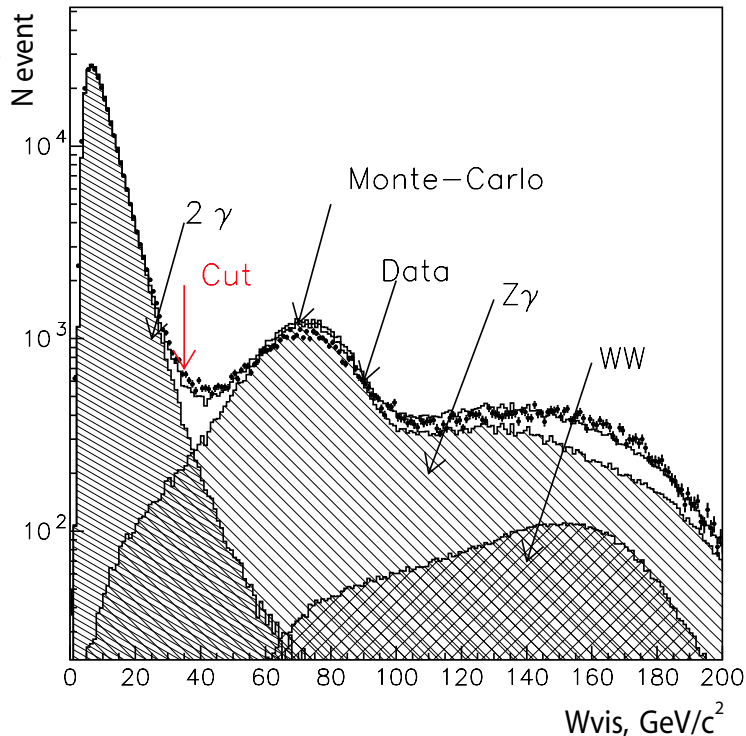GeV/c^2 rejects the major part of the non-two-photon events.

Figure 2: W_{vis} distributions for the LEP II DELPHI data and for the simulated $\gamma\gamma \rightarrow$ hadrons, $e^+e^- \rightarrow Z^0\gamma$, $e^+e^- \rightarrow W^+W^-$ and the sum of all above Monte-Carlo contributions

A total of 274 510 events remain in the data sample after applying all these cuts. The main background comes from the process $e^+e^- \rightarrow Z\gamma$ and amounts to $\sim$1.2% of the selected $\gamma\gamma$ events. The backgrounds from the $e^+e^- \rightarrow W^+W^-$ and other processes are negligible, as seen in Fig. 2.

J/ψ candidates have been selected using the $\mu^+\mu^-$ decay channel. For the muon pair selection the following criteria were imposed:

(n) at least two charged particle tracks with zero net charge should satisfy the standard DELPHI muon-tagging algorithm [5] or be identified as muons by the hadronic calorimeter;

(o) the tracks should not come from any reconstructed secondary vertex or be identified as a kaon, proton or electron by the standard DELPHI identification packages;

3 Inclusive J/ψ Production

In Fig. 3 we give the invariant mass distribution for pairs of identified $\mu^+\mu^-$ selected as outlined in the previous section. It is seen that the J/ψ is produced over little background. A least squares fit to the $M(\mu^+\mu^-)$ distribution with a Gaussian for the signal and a second order polynomial for the background gives the following results:

$$
\begin{aligned}
J/\psi \text{ mass:} && M &= 3119 \pm 8 && \text{MeV}/c^2 \\
J/\psi \text{ width:} && \sigma(\text{obs}) &= 35 \pm 7 && \text{MeV}/c^2
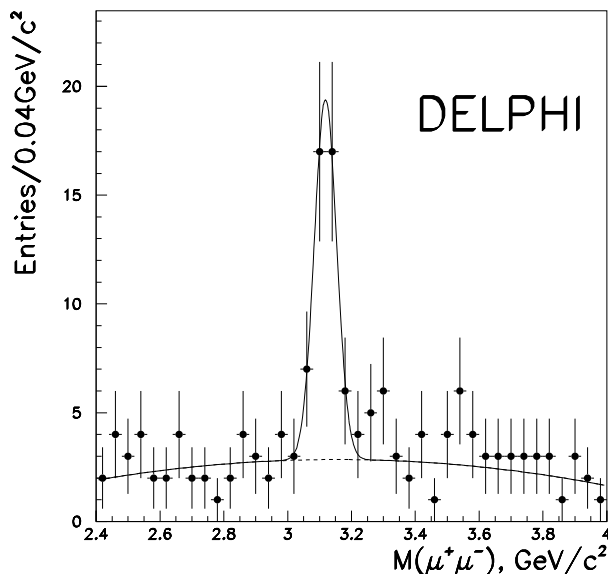\end{aligned}
$$

3

Figure 3: $M(\mu^+\mu^-)$ distribution from the LEP II DELPHI data. The solid curve corresponds to a Gaussian fit over a second order polynomial background.

The observed width of the peak is consistent within errors with the invariant mass resolution of the pair of charged particle tracks in the mass region around $3\,\mathrm{GeV}/c^2$. The number of observed events from the fit is $N(J/\psi) = 36 \pm 7$. If we take the L3 result[6] on beauty cross-section from $\gamma\gamma$ events and the PDG value[7] for the branching ratio of beauty hadrons to J/ψ, the expected number of $J/\psi \rightarrow \mu^+\mu^-$ from beauty hadrons is 2.1 ± 0.6. The backgrounds from the processes $e^+ + e^- \rightarrow Z + \gamma \rightarrow J/\psi + X$ and $\gamma + \gamma \rightarrow \chi_{c2} \rightarrow J/\psi + \pi^+ + \pi^- + \pi^0$ are less than 0.20 and 0.30 events, respectively. According to our selection criteria the system X contains at least two charged particle tracks, hence we do not consider such sources of J/ψ production as $\gamma + \gamma \rightarrow \chi_{c2} \rightarrow J/\psi + \gamma$. We checked that in the four-prong events with $J/\psi \rightarrow \mu^+\mu^-$ candidates there is no photon conversions.

We used the PYTHIA 6.156 generator [8] to estimate the efficiency. The generated events were passed through the simulation package of the DELPHI detector [9] and then processed with the same reconstruction and analysis programs as the real data. There is a substantial fraction of PYTHIA events where J/ψ's are produced just as a simple fusion of two photons because there is not enough phase space to produce additional particles. We do not use such events. The process where both photons are VDM photons we will call as 'diffractive' and the process without VDM photons we will call as 'resolved'.

The characteristics of the J/ψ production are shown on Fig.4 to Fig.8. For all these figures, the background was estimated from the analysis of the $M(\mu^+\mu^-)$ spectrum for every bin of a given distribution and was statistically subtracted.

Fig. 4 shows the $p_T^2(J/\psi)$ distribution. As expected, the PYTHIA prediction for the $p_T^2(J/\psi)$ distribution is more sharply peaked near zero for the diffractive MC events (see Fig.1 (a)) than for the 'resolved' MC events (see Fig.1 (b)). We fitted the experimental
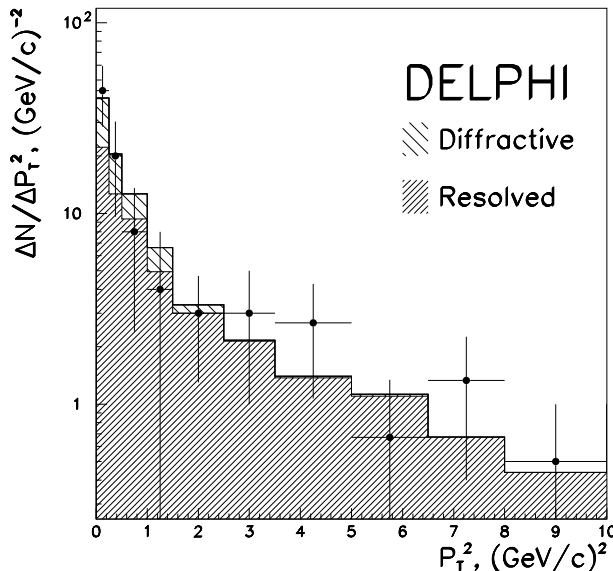
Figure 4: $p_T^2(J/\psi)$ distribution from the LEP II DELPHI data, shown as points with error bars. The histogram is a composite of the renormalized 'resolved' and 'diffractive' processes from PYTHIA (see text).

$p_T^2(J/\psi)$ distribution as a function of the two categories of MC PYTHIA events

$$\frac{\mathrm{d}N}{\mathrm{d}p_T^2} = f \cdot \left.\frac{\mathrm{d}N}{\mathrm{d}p_T^2}\right|_{\text{Diffractive}} + (1 - f) \cdot \left.\frac{\mathrm{d}N}{\mathrm{d}p_T^2}\right|_{\text{Resolved}} \tag{5}$$

which gives $f = (26 \pm 22)\%$ (PYTHIA distributions in Fig 4 are normalized to the data). The PYTHIA study tells us that the experimental efficiencies are very different for the two categories:

$$\begin{aligned} \epsilon(\text{diffractive}) &= (0.98 \pm 0.04)\% \\ \epsilon(\text{resolved}) &= (3.87 \pm 0.09)\% \end{aligned} \tag{6}$$

According to PYTHIA, about one-half of all the $\gamma\gamma$ events with $J/\psi \to \mu^+\mu^-$ are produced with the charged particle tracks at polar angles below 10 degrees, so that they are invisible to the DELPHI detector. The individual efficiencies as a function of p_T^2 are given in Fig. 5. Some insight may be gained into these efficiencies if they are broken down into products of two factors, as follows:

$$\begin{aligned} \epsilon(\text{diffractive}) &= \epsilon_{\gamma\gamma}(\text{diffractive}) \times \epsilon_{J/\psi \to \mu^+\mu^-}(\text{diffractive}) \\ \epsilon(\text{resolved}) &= \epsilon_{\gamma\gamma}(\text{resolved}) \times \epsilon_{J/\psi \to \mu^+\mu^-}(\text{resolved}) \end{aligned} \tag{7}$$

where $\epsilon_{\gamma\gamma}$ is the efficiency for the process $\gamma\gamma \to J/\psi + X$ and $\epsilon_{J/\psi \to \mu^+\mu^-}$ is that for $J/\psi \to \mu^+\mu^-$. As expected, the latter is relatively process-independent

$$\begin{aligned} \epsilon_{J/\psi \to \mu^+\mu^-}(\text{diffractive}) &= (37.0 \pm 1.5)\% \\ \epsilon_{J/\psi \to \mu^+\mu^-}(\text{resolved}) &= (32.1 \pm 0.7)\% \end{aligned} \tag{8}$$

It is clear, therefore, that the difference in efficiency in (6) is mostly due to $\epsilon_{\gamma\gamma}$—this is highly process-dependent and hence model-dependent.

5

The overall experimental efficiency is

$$\frac{1}{\epsilon} = \frac{f}{\epsilon(\text{diffractive})} + \frac{1-f}{\epsilon(\text{resolved})} \qquad (9)$$

which gives $\epsilon = (2.19^{+1.27}_{-0.59})\%$. Under the assumption that PYTHIA captures the kinematical features of the resolved and diffractive processes—but not their absolute cross-sections—the cross-section for inclusive J/ψ production is

$$\sigma = N(J/\psi) \cdot (Br \cdot \mathcal{L} \cdot \epsilon)^{-1} = 45.3 \pm 18.9 \text{ pb} \qquad (10)$$

where $Br = (5.88 \pm 0.10)\%$ is the branching ratio for $J/\psi \rightarrow \mu^+\mu^-$ [7] and $\mathcal{L} = 617\,\text{pb}^{-1}$ is the total integrated luminosity. The quoted error reflects only that associated with the visible part of the spectra; in particular, it does not include the uncertainties inherent to the PYTHIA program.
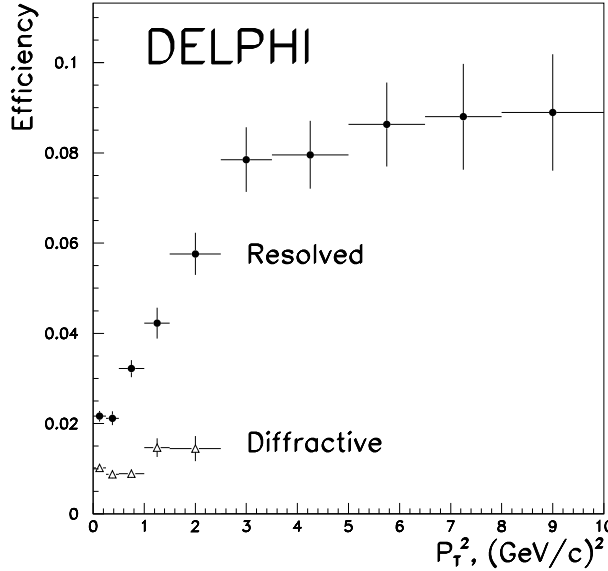
Figure 5: Efficiencies for resolved and diffractive processes as functions of p_T^2.

Because of the model-dependent aspect of this analysis (see, for example, the efficiencies given in (6)), it is of interest to quote the 'visible' cross-section. Substituting $\epsilon_{J/\psi \rightarrow \mu^+\mu^-}(\text{diffractive})$ and $\epsilon_{J/\psi \rightarrow \mu^+\mu^-}(\text{resolved})$ for $\epsilon(\text{diffractive})$ and $\epsilon(\text{resolved})$—respectively—in (9), the 'visible' cross-section can be calculated; it is

$$\sigma_{\text{vis}} = 2.99 \pm 0.58(\text{stat}) \pm 0.10(\text{syst}) \text{ pb} \qquad (11)$$

The main source of systematic uncertainty comes from the determination of the relative fractions of resolved and diffractive events which have different efficiencies (8). Following the same argument, we also give the 'visible' production rate $\langle n \rangle$ for J/ψ production

$$\langle n \rangle = N(J/\psi) \cdot \left(N_t \cdot Br \cdot \epsilon_{J/\psi \rightarrow \mu^+\mu^-} \right)^{-1} = (6.7 \pm 1.3(\text{stat}) \pm 0.2(\text{syst})) \times 10^{-3} \qquad (12)$$

where N_t is the data sample for the $\gamma\gamma$ selection as given in the previous section, i.e. $N_t = 274\,510$.

The rapidity distribution for the J/ψ is shown in Fig. 6. The PYTHIA MC events have been combined using the same fraction f found in (5) and then normalized to the observed number of events in $0 < |y| < 2.0$. The same techniques have been used to compare the experimental distributions of $M(J/\psi + X)$, $M(X)$, the charged and total multiplicities $[N_{ch}(X)$ and $N_{tot}(X)]$, in Fig.7 a, b, c, and d. There is fair agreement within statistics between the shapes of our measured distributions and the PYTHIA predictions (using the best fit as found in (5) for the relative content of diffractive and resolved events and renormalizing the PYTHIA prediction to the number of observed events).
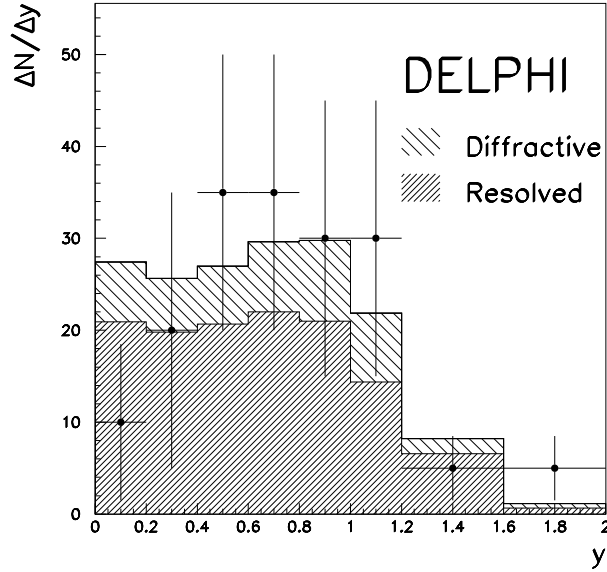
Figure 6: $|y|$ distribution for the J/ψ from the LEP II DELPHI data, shown as points with error bars. The histogram is a composite of the renormalized 'resolved' and 'diffractive' processes from PYTHIA (see text).

The acceptance-corrected distributions in $\cos\theta$ where θ is the helicity angle of μ^+ in the rest frame of $J/\psi \to \mu^+\mu^-$ are shown in Figs.8 (a–c), along with the results of a fit to the form $(1 + a\cos^2\theta)$. The fitted parameters are $a = -0.93 \pm 0.57$ for the total sample (a), $a = -1.76 \pm 0.53$ for $p_T^2(J/\psi) < 1.0$ (GeV/c^2) (b) and $a = 0.71 \pm 1.33$ for $p_T^2(J/\psi) > 1.0$ $(\text{GeV}/c)^2$ (c). These results indicate that the J/ψ's are produced with little polarization at high $p_T^2(J/\psi)$, where the main contribution comes from the resolved processes.
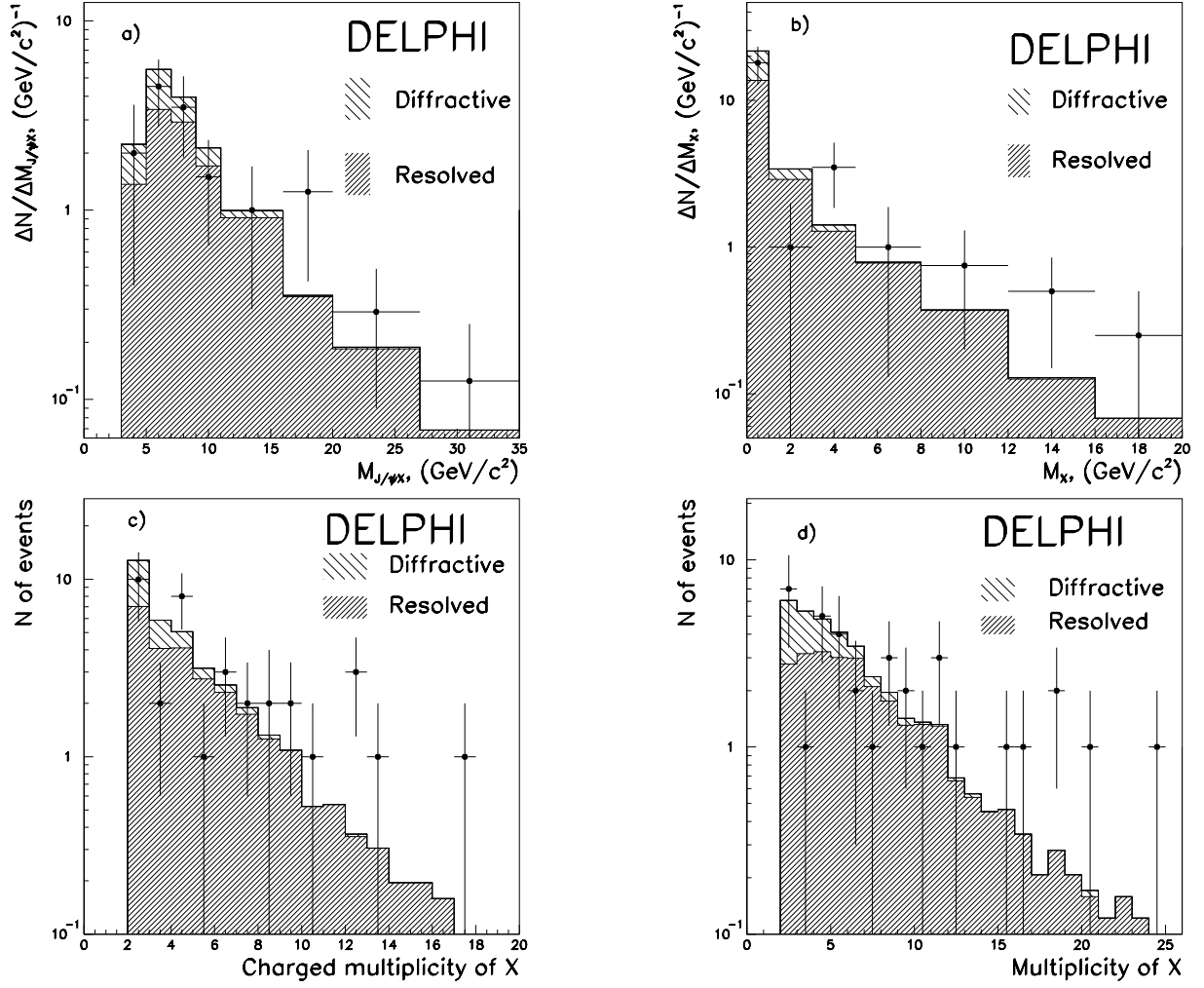
7

Figure 7: Visible distributions of $M(J/\psi + X)$ (a), $M(X)$ (b), charged (c) and total (d) multiplicities of the X system. Each histogram is a composite of the renormalized 'resolved' and 'diffractive' processes from PYTHIA (see text).
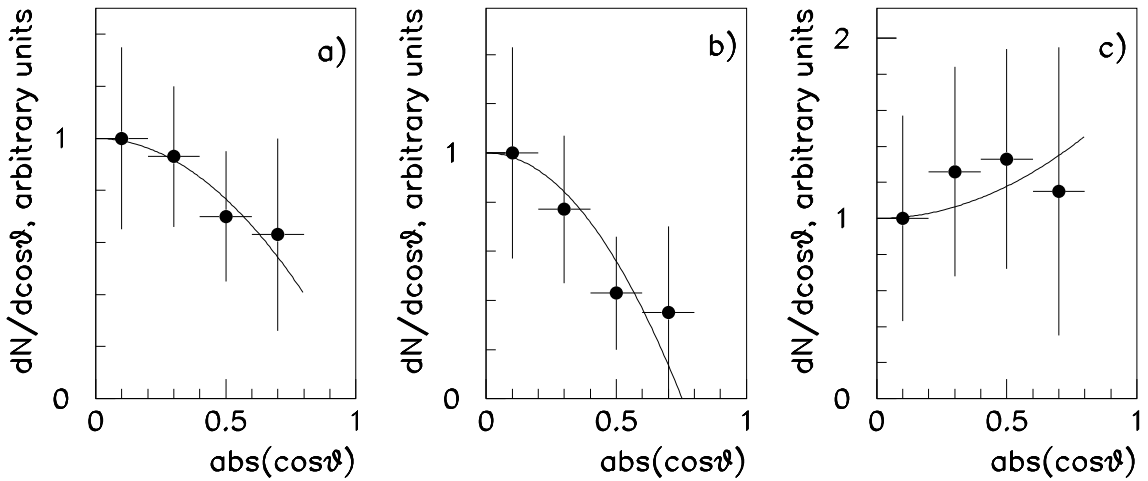

Figure 8: Acceptance-corrected distributions in $\cos\theta$ where θ is the helicity angle of μ^+ in the rest frame of $J/\psi \to \mu^+\mu^-$. The figures (a–c) correspond to the total sample (a), the subsamples with $p_T^2(J/\psi) < 1.0$ (GeV/c)^2 (b) and $p_T^2(J/\psi) > 1.0$ (GeV/c)^2 (c).

4   Conclusions

We have studied the inclusive J/ψ production from $\gamma\gamma$ collisions. The data have been taken by the DELPHI collaboration during the LEP II phase, i.e. $\sqrt{s}$ of the LEP machine ranged from 161 to 207 GeV. A clear signal from the reaction $\gamma\gamma \rightarrow J/\psi + X$ is seen.

The inclusive cross-section is estimated to be $\sigma(J/\psi + X) = 45.3 \pm 18.9$ pb. Based on a study of the p_T^2 distribution of different types of $\gamma\gamma$ processes in the PYTHIA program, we conclude that some $(74\pm22\,)\%$ of the observed J/ψ events are due to the 'resolved' photons, the dominant contribution of which is derived from a gluon content of the photon [3].

The distributions in $p_T^2(J/\psi)$, y and $\cos\theta$ (for μ^+ in the rest frame of $J/\psi \rightarrow \mu^+\mu^-$) are presented. In addition, a study is given of the characteristics of the system X. All distributions appear to be well reproduced within statistics by the renormalized combination of the fitted 'resolved' and 'diffractive' contributions.

Acknowledgements

References

[1] 'Physics at LEP2,' edited by G. Altarelli, T. Sjöstrand and F. Zwirner, CERN96-01 (Vol. 1), Feb 1996.
See Section 7 (heavy-quark physics), p. 330, in the chapter on $\gamma\gamma$ physics.

[2] J.J. Sakurai and D. Schildknecht, Phys. Lett. **B40** (1979) 121;
I. F. Ginzburg and V.G. Serbo, Phys. Lett. **B109** (1982) 231.

[3] M. Klasen *et al.*, Nucl. Phys. **B609** (2001) 518;
M.Klasen *et al.*, hep-ph/0112259;
R. M. Godbole *et al.*, Phys. Rev. **D65** (2002) 074003;
E. L. Berger and D. Jones, Phys. Rev. **D23** (1981) 1521;
H. Jung, G. A. Schuler and J. Terrón, Int. J. Mod. Phys. **A7** (1992) 7955
B. Naroska, Nucl. Phys. B (Proc. Suppl.) **82** (2000) 187.

[4] P. Aarnio *et al.*, DELPHI Collab., Nucl. Inst. Meth. **A303** (1991) 233.

[5] P. Abreu *et al.*, DELPHI Collab., Nucl. Inst. Meth. **A378** (1996) 57.

[6] R. Acciarri *et al.*, L3 Collab., Phys. Lett. **B503** (2001) 10.

[7] Particle Date Group, Eur. Phys. J. **C15**, (2000) 1.

[8] T. Sjöstrand *et al*, Comput. Phys. Comm. **135** (2001) 238.

[9] Delphi notes DELPHI 89-15 PROG 130 and DELPHI 89-68 PROG 143.